Analytical study of vertical Hall (VH)-devices using an adapted conform mapping technique.

P.A. Besse, Ch. Schott and R.S. Popovic

Institute of Microsystems, EPFL-DMT, CH-1015 Lausanne, Switzerland.
Phone: +41-21- 693 6766; Fax: +41-21- 693 6670; e-mail: besse@epfl.ch

ABSTRACT

We adapt the conform mapping technique to the analytical calculation of two dimensional vertical Hall (VH)-devices with five electrical contacts. With our new method the finite size of the two output current electrodes is taken into account. The mapping technique has been extended to VH-devices embeded in a well or in a guard-ring. Different cases, all based on a typical VH-device, have been studied to illustrate the potentialities of the method. We calculate the geometry factor, the series resistance as well as the current unbalance between both output current electrodes. Such accurate calculations are especially required in order to understand the efficient linearization schemes recently developed for such VH-devices.

Keywords: Magnetic sensor, Hall-devices, Conform mapping, Geometry factor, Series resistance.

INTRODUCTION

The Hall effect is widely used for magnetic sensor applications [1]. Vertical Hall (VH)-devices have gained in interest due to their very long-term stability. Recently efficient linearization schemes have been experimentally applied on these devices [2]. By choosing an appropriate design, it was shown that geometry-related and magnetoresistive nonlinearities can be used for mutual cancellation. In this paper we concentrate on an analytical study of the influences of geometrical parameters on the VH-device in two dimensions. We adapt the well-known conform mapping technique [1],[3],[4],[5] in order to take into account the finite size of the output current electrodes (Fig.1). Furthermore we extend the method to VH-devices embeded in a well or in a guard-ring. Our analytical analysis permits to accurately calculate the geometry factor, the series resistance as well as the current unbalance between both current outputs.

VH-DEVICES OF INFINITE EXTENSION

Conform mapping

We consider first the two dimensional VH-device of infinite extension (Fig.1).The active region is the half-plane below the real axis. The output current electrodes have a finite width d. Note that a normalization of the complex plane can be applied at any time, since this is a conform transformation. First, the w-plane is normalized so that the input current electrode is located between w_6=-1 and w_7=+1.

We then use an adapted Schwarz-Christoffel transformation [6],[7] that maps the half-plane w into the skew parallelogram of fig.2 located in the z-plane.

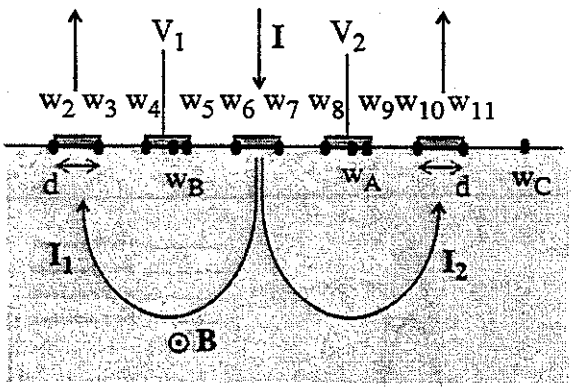

Fig: 1 Schematic view of a 2D vertical Hall-device located in the complex w-plane. The magnetic field B is perpendicular to the plane. The active area of the sensor is dotted. The Hall-voltage is the difference V_1-V_2. d= width of the ouput curent electrodes.

This transformation is explicitely given by:

$$z^* = H \cdot \int_0^{w^*} \frac{(u-w_A)(u-w_B)(u-w_C)}{f_1 \cdot f_2 \cdot f_3} \cdot du$$

with:

$$f_1 = (u-w_7)^{\alpha_+}(u-w_8)^{\alpha_-}(u-w_9)^{\alpha_+}$$

$$f_2 = (u-w_6)^{\alpha_-}(u-w_5)^{\alpha_+}(u-w_4)^{\alpha_-}$$

$$f_3 = (u-w_2)^{\alpha_-}(u-w_3)^{\alpha_+}(u-w_{10})^{\alpha_-}(u-w_{11})^{\alpha_+}$$

$$\alpha_\pm = \frac{1}{2} \pm \frac{\beta}{\pi}$$

with β the Hall angle given by: $\tan(\beta) = \mu \cdot B$, where μ is the mobility. The symbole * indicates the conjugate complex. The points w_A, w_B and w_C are chosen so that the sides (z_{10},z_7) (z_3,z_6) and (z_3,z_{10}) of the parallelogram are on straight lines, respectively. The normalization constant H can take any value, but in this paper we use:

$$H = -\frac{w_{10} \cdot e^{-i\left(\frac{\pi}{2}-\beta\right)}}{w_C}$$

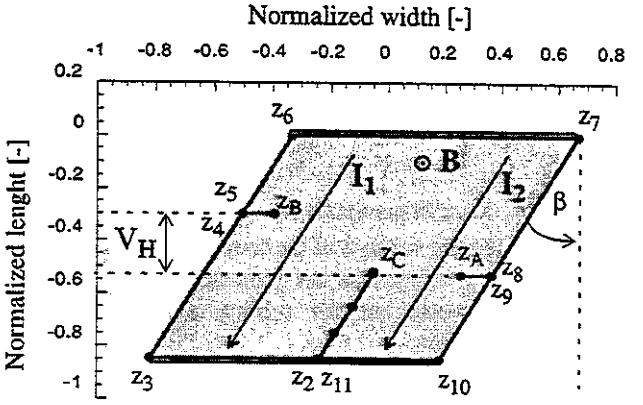

Fig.2: Schematic view of the resulting skew Hall-device after conform mapping. The input and output current electrodes cover the entire sides of the parallelogram. The Hall angle β is defined by $\tan(\beta)= \mu.B$. The Hall-voltage V_H can be directly determined. The current lines as well as the equipotential lines are parallel to the sides of the active area (dotted). In this example the Hall angle β is defined as positive. (β=+30°).

After transformation (fig.2) the equipotential lines are horizontal and equidistant. The electrical field is perpendicular to all five electrodes. Now the vertical Hall-device can be analysed as the planar Hall-plate [3]. In the z-plane the relevant parameters of the Hall device can be easy determined using:

$$\frac{V_H}{I} = \frac{\rho}{s} \cdot G \cdot \tan(\beta) \qquad \text{and:}$$

$$\frac{V_H}{V} = \frac{\rho}{s} \cdot \frac{G}{R} \cdot \tan(\beta)$$

with ρ = material's resistivity, s = thickness in the third direction, G = geometry factor, R = series resistance. In this paper we use the value ρ/s= 2000Ω for all the examples.

The geometry factor, the series resistance and the current unbalance can be determined by elementary calculations. We get for the geometry factor G and the resisitivity R:

$$G = \frac{1}{|\sin(\beta)|} \cdot \frac{\big||z_8-z_7|-|z_5-z_6|\big|}{|z_7-z_6|}$$

$$R = \frac{\rho}{s} \cdot \frac{1}{|\cos(\beta)|} \cdot \frac{|z_{10}-z_7|}{|z_7-z_6|}$$

The current unbalance is defined as:

$$\frac{I_2}{I_1} = \frac{|z_{11}-z_{10}|}{|z_2-z_3|}$$

Compared with the well-known conform mapping [3], the new transformation introduces a third incision (z_{11}, z_C, z_2) in order to take the finite width of the two outpout current electrodes into account. After mapping, these electrodes are unified and they cover completely the side of the skew parallelogram. This considerably simplifies the calculation of the current flow and of the voltage distribution in the transformed device, leading to the simple relations described above for R, G and for the current unbalance. Note that the description of other properties of VH-devices can benefit of such a transformation.

Using the fact that z_6 and z_7 are on the real axis, the three above relations can be rewritten as function of z_5, z_8 and z_2 only. We get:

$$G = \left|\frac{1}{\sin(\beta)\cos(\beta)}\right| \frac{|Im(z_5)-Im(z_8)|}{|Re(z_8)-Re(z_5)+(Im(z_5)-Im(z_8))\tan(\beta)|}$$

$$R = \frac{\rho}{s} \cdot \frac{1}{\cos^2(\beta)} \frac{|Im(z_2)|}{|Re(z_8)-Re(z_5)+(Im(z_5)-Im(z_8))\tan(\beta)|}$$

$$\frac{I_2}{I_1} = \frac{|Re(z_8)-Re(z_2)-(Im(z_8)-Im(z_2))\tan(\beta)|}{|Re(z_2)-Re(z_5)+(Im(z_5)-Im(z_2))\tan(\beta)|}$$

Not the full skew parallelogram of Fig.2 has to be computed, only the calculation of the three points z_5, z_8 and z_2 is required to determine characteristical parameters such as the geometry factor G, the series resistivity R and and the current unbalance I_2/I_1.

Results

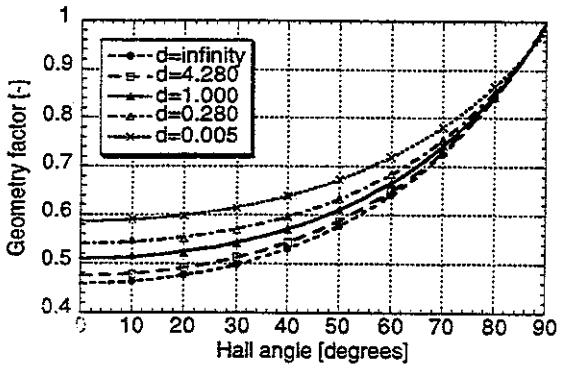

Fig.3: Analytic calculations of the geometry factor of vertical Hall devices as function of the Hall angle. The device is symmetric and normalized such that w_7=1. (Fig.1). d = width of the output current electrodes. w_8=1.68, w_9=2.68, w_{10}=3.72.

In order to illustrate the potentialities of the above conform mapping technique, we first study the influence, on the geometry factor G, of the finite normalized width d of the output current electrodes (fig.3). We consider typical vertical Hall-devices as used in [2]. A decreasing width increases the factor G of more than 25% for this particular case.

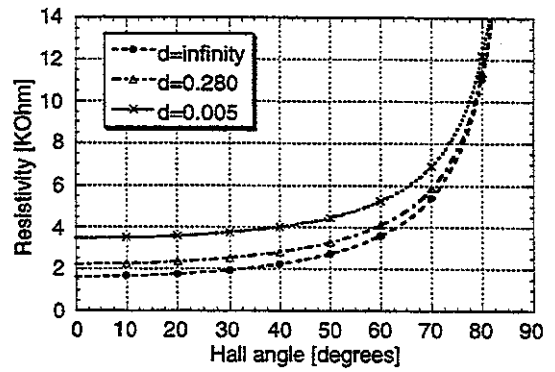

Fig.4: Analytic calculations of the series resistance of vertical Hall devices as function of the Hall angle, using the same geometry as for Fig.3. (ρ/s= 2000Ω)

As already pointed out in [3] the geometry factor can be fitted by:

$$G \equiv G_0 + a \cdot \frac{\beta}{\tan(\beta)} + b \cdot \left(\frac{\beta}{\tan(\beta)}\right)^2$$

where G_0, a, b are fit parameters.

For the same geometry the serie resistance and the current unbalance can be calculated. The results are shown on Fig. 4 and Fig.5.

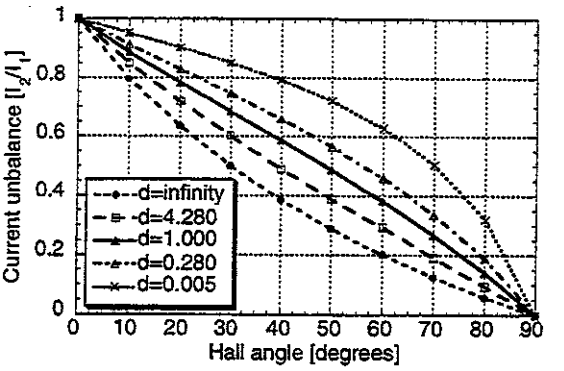

Fig.5: Analytic calculations of the current unbalance of vertical Hall devices as function of the Hall angle using the same geometry as on Fig.3.

Now the series resistance is fitted by:

$$R \equiv R_0 + A \cdot \frac{\tan(\beta)}{\beta} + B \cdot \left(\frac{\tan(\beta)}{\beta}\right)^2$$

where R_0, A, B are fit parameters.

Decreasing the width d of the output current electrodes has the tendency to increase the geometry factor as well as the series resistance, but the current is better balanced between both outputs.

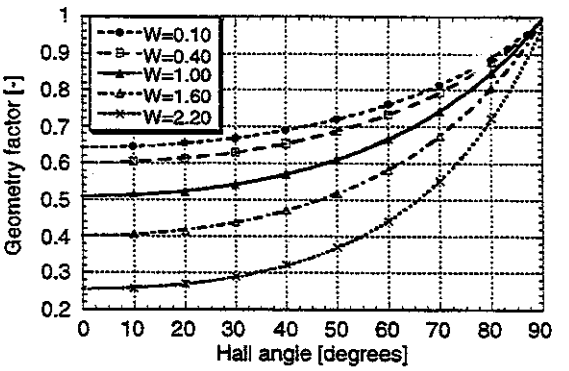

Fig.6: Analytic calculations of the geometry factor of vertical Hall devices as function of the Hall angle. The device is symmetric (Fig.1) and normalized such that w_7=1.0. W= width of voltage electrodes= $|w_9-w_8|$. $(w_8+w_9)/2$=2.18, w_{10}=3.72, w_{11}=4.72.

Other parameters that strongly influence the geometry factor are the width W of the voltage electrodes as well as the position of these electrodes between the in- and output current electrodes. We study these influences using again the typical device [2] as reference.

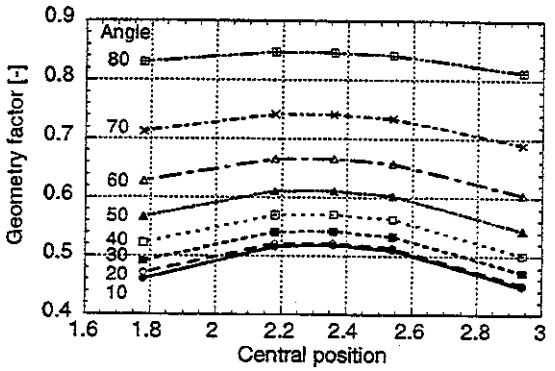

Fig. 7: Analytic calculations of the geometry factor of vertical Hall devices as function of the central position of the voltage electrodes.The device is symmetric and normalized such that w_7=1. The voltage electrode width W=1.0. w_{10}=3.72, w_{11}=4.72. The central position is defined by $(w_8+w_9)/2$. The Hall angle varies between 10° and 80°.

A larger width of the voltage electrodes strongly influences the current behavior in the device. This reduces the geometry factor drastically (Fig.6). An optimum position of the voltage electrodes is in the middle between the in- and output current electrodes, but this is not very critical (Fig.7).

Up to now we have studied VH-devices of infinite extension. In practical applications, the active area of the sensor is limited. The device is realized in a well or in the middle of a guard-ring. As shown in the two next sections, both cases can be conformed mapped into the case of a VH-device with infinite extension, allowing us to solve both problems in the same way as in this section.

VH-DEVICES IN A WELL

Conform mapping

We consider the VH-device of Fig.8, embeded in a well. The active area is limited to the dotted surface. We admit that no current is living this region except by the output current electrodes. Without lack of generality, the t-plane is normalized so that t_1 and t_{12} are on the real axis and symmetric around the origin. The problem is reduced to the one described in the previous section by applying another conform mapping.

The t-plane is transformed into the $\overline{w}$-plane where the device is located in the whole half-plane below the real axis. The point t_{14} goes to infinity along the real axis. This conform mapping, using the Jacobian elliptical [8] function sn, is given by:

$$\overline{w} = \mathrm{sn}\left[\frac{t}{A},\ k^2\right] \qquad \text{with:}$$

$$A = \frac{|t_1 - t_{12}|}{2 \cdot F\langle \mathrm{asin}(1)|k^2\rangle}$$

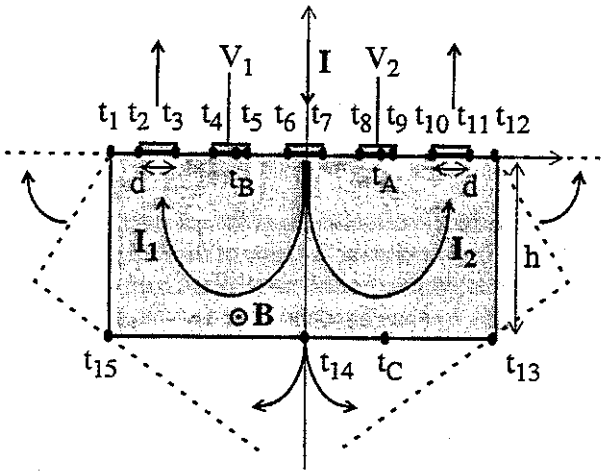

Fig.8: schematic view of the vertical Hall-device, embeded in a well. The active area of the sensor is dotted. The magnetic field B is perpendicular to the plane. The Hall-voltage V_H is the difference V_1-V_2. In a first step the device is conform mapped into the half-plane below the real axis, the point t_{14} going to infinity. d= width of the output current electrodes.

The parameter $k \in [0,1]$, determined from the aspect ratio of the dotted area of Fig.8, is solution of the equation:

$$\frac{|t_1 - t_{12}|}{2 \cdot |t_{12} - t_{13}|} = -\frac{F\langle \mathrm{asin}(1)|k^2\rangle}{Im(F\langle \mathrm{asin}(1/k)|k^2\rangle)}$$

where $F\langle\phi|m\rangle$ is the elliptic integral of the first kind [8].

Finally, the plane $\overline{w}$ is normalized to get the w-plane of previous section by: $w = (2 \cdot \overline{w})/|\overline{w}_7 - \overline{w}_6|$. The input current electrode is now located between w_6=-1 and w_7=+1.

Results

As example, we take the typical VH-device of [2] and consider the influence of a well, limiting the area of the active region. Especially we vary the depth h of the well.

Reducing the depth of the well, will push the current against the surface. Therefore the voltage electrodes will have much more influence, this leads to a reduction of the geometry factor (Fig.9).

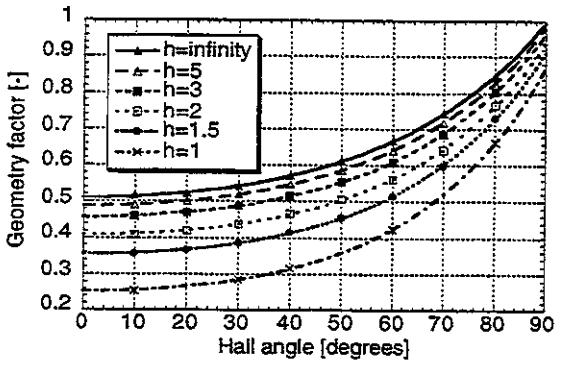

Fig. 9: Analytic calculations of the geometry factor of vertical Hall devices as function of the Hall angle. The device is symmetric and normalized such that t_7=1 (Fig.8). h = height of the well. t_8=1.68, t_9=2.68, t_{10}=3.72, t_{11}=4.72, t_{12}=6.0.

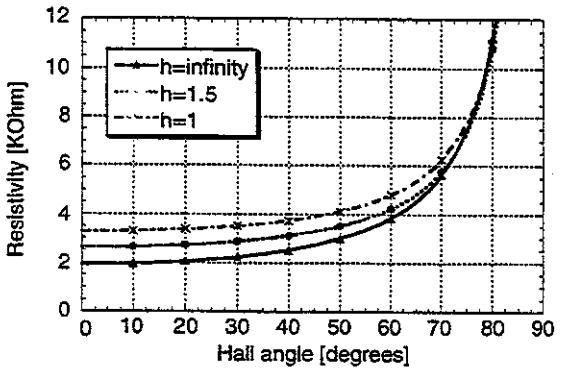

Fig. 10: Analytic calculations of the series resistance of vertical Hall devices as function of the Hall angle. h = height h of the well. The device is the same as on Fig.9. (ρ/s= 2000Ω).

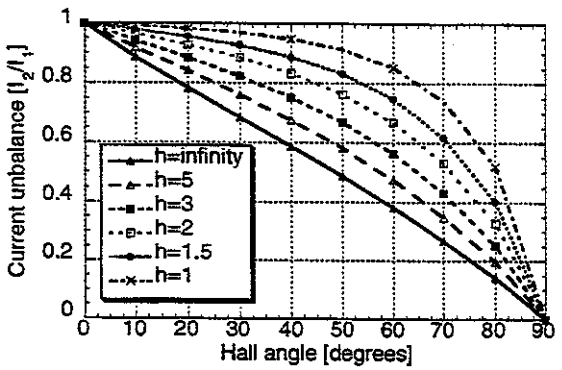

Fig.11: Analytic calculations of the current unbalance of vertical Hall devices as function of the Hall angle. h = height h of the well. The device is the same as on Fig.9.

For the same transformation, the cross-section where the current is flowing is reduced, resulting in an increase of the series resistance (Fig.10). The resulting current unbalance is shown on Fig.11. The current is better balanced between both output electrodes for a thinner well.

VH-DEVICES IN A GUARD-RING

Conform mapping

In this section we analyse the influence of a guard-ring, like on Fig.12. Again using a Schwarz-Christoffel transformation we can relate this geometry to the case of Fig.1.

First the device of Fig12 is conformally related to the $\overline{w}$-plane by the transformation:

$$t = C_0 \cdot \int_0^{\overline{w}} \frac{\sqrt{(u-\overline{w}_{13})(u+\overline{w}_{15})(u-\overline{w}_{16})(u+\overline{w}_{17})}}{\sqrt{(u-1)(u+1)(u-\overline{w}_{18})(u+\overline{w}_{19})}} \cdot du$$

From symmetry considerations we get: $\overline{w}_{15}=-\overline{w}_{13}$, $\overline{w}_{17}=-\overline{w}_{16}$ and $\overline{w}_{19}=-\overline{w}_{18}$.

We use the normalization $\overline{w}_{12}=-\overline{w}_1=1$.

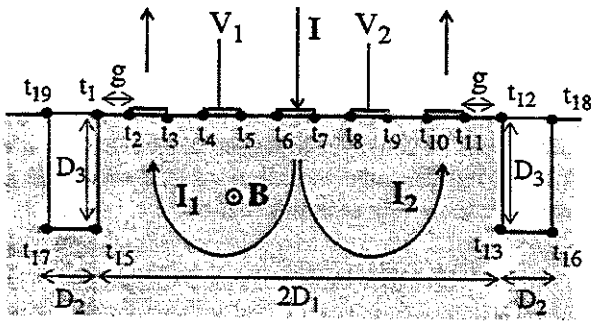

Fig12: Schematic view of a 2D vertical Hall-device located in the complex t-plane. The magnetic field is perpendicular to the plane. The active area of the sensor is dotted. The guard-ring is symmetric and will be defined by the values D_1, D_2 and D_3. g is the gap between the guard-ring and the output current electrodes.

The four parameters C_0, $\overline{w}_{13}$, $\overline{w}_{16}$ and $\overline{w}_{18}$ are given by:

$$t_{12} = D_1$$

$$Im(t_{18}) = 0$$

$$D_1 \cdot |Im(t_{13})| = D_3 \cdot |Re(t_{13})|$$

$$D_1 \cdot |Re(t_{16}) - Re(t_{13})| = D_2 \cdot |Re(t_{13})|$$

Then the case of Fig.1 can be generated by scaling the $\overline{w}$-plane by: $w = (2 \cdot \overline{w}) / |\overline{w}_7 - \overline{w}_6|$.

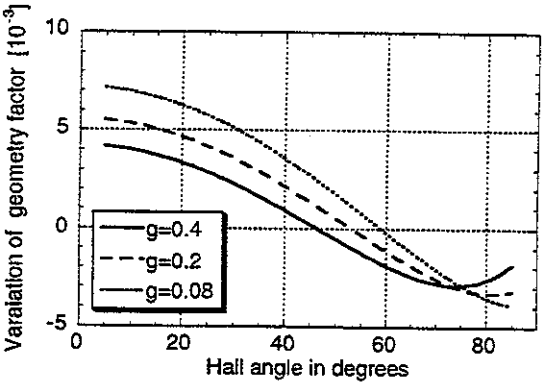

Fig.13: Variations of the geometry factor of the VH-devices of Fig.12, compared to VH-devices without guard-ring. The device is symmetric and normalized such that t_7=1. g= gap between guard-ring and electrodes. t_8=1.68, t_9=2.68, t_{10}=3.72, t_{11}=4.72.

Results

As example of this transformation, we consider the variation of the gap g between the guard-ring and the output current electrodes (Fig.12). Since such a guard-ring introduces only week perturbations of the device behavior, we calculate the variations of the geometry factor compared to the case without guard-ring (Fig.13).

CONCLUSION

In conclusion, we have adapted the conform mapping technique to the analytic calculations of geometry factor, series resistance and current unbalance in vertical Hall-devices with five electrical contacts. The influence the finite width of the output current electrodes has been taken into account. Furthermore the method has been extended to take into account the influence of a well or of a guard-ring limiting the active area.

Such calculations are required in order to compensate the magneto-resistive effect and to accurately linearize the Hall sensor using the technique developed in [2].

A series of examples illustrates the potentialities of the proposed analytical method. We have only consider the cases of symmetrical devices, but the method itself can be used to take asymmetries into account.

ACKNOWLEDGEMENTS

This work was partially supported by the swiss priority program MINAST 3.03 Magsens.

REFERENCES

[1] R.S. Popovic: «Hall effect devices», Adam Hilger series on sensors, 1991. ISBN 0-7503-0096-5.

[2] Ch. Schott and R.S. Popovic: "Linearizing integrated hall devices", Transducers'97, Chicago, USA, June 16-19, 1997, paper: 2B1.05P.

[3] W. Versnel: "The geometrical correction factor for a rectangular Hall plate" J. Appl. Phys. 53 (7), July 1982, pp.4980-4986.

[4] W. Versnel: "Analysis of symmetrical Hall plates with finite contacts" J. Appl. Phys. 52 (7), July 1981, pp.4659-4666.

[5] J. Haeusler: "Exakte Lösungen von Potentialproblemen beim Halleffekt durch konforme Abbildung", Solid-State Electronics, vol.9, 1966, pp. 417-441.

[6] I.N. Bronstein and K.A. Semendjajew: «Taschenbuch der Mathematik», Verlag Harri Deutsch, 1993. ISBN 3-8171-2001-X.

[7] Cinag C. Mei: "Mathematical analysis in engineering" Cambridge University Press, 1995, ISBN 0-521-46053-0.

[8] M. Abramowitz and I.A. Stegun: "Handbook of mathematical functions", Dover Publications, Inc., New-York, 1965, ISBN: 0-486-61272-4.